Stripe and line textures in the $B2$ phase of bent-shape molecules in samples with polar surface anchoring

Lubor Lejček,* Vladimíra Novotná, and Milada Glogarová
Institute of Physics, Academy of Sciences of the Czech Republic, Na Slovance 2, CZ-182 21 Prague 8, Czech Republic
(Received 23 June 2011; published 1 December 2011)

In the $B2$ phase formed by bent-shaped molecules a dense line texture is frequently observed. For the texture description a model is proposed consisting of a periodic system of anticlinic antiferroelectric bulk domains with opposite chiralities separated by π walls in which polarization rotates. The bulk domains are situated between layers of synclinic ferroelectric phase near the upper and lower surfaces. In the surface layers induced by polar anchoring domains of opposite chirality are separated by defect lines. Under the electric field the ferroelectric layer near one sample surface is growing against the antiferroelectric structure in the sample bulk and the stripe texture is fading out, but still in the saturated field surface lines or walls persist separating ferroelectric domains of opposite chirality. The proposed model is adapted also for a case when the anticlinic antiferroelectric structure in the sample bulk is sandwiched between anticlinic ferroelectric layers near the surfaces. In that case the applied electric field eliminates all the lines because the resulting anticlinic ferroelectric structure is racemic, with no chiral domains.

DOI: 10.1103/PhysRevE.84.061701 PACS number(s): 61.30.Dk, 61.30.Hn

I. INTRODUCTION

Liquid crystals composed of bent-shaped molecules have become an important subfield in the investigation of mesogenic compounds [1,2]. Packing of bent-shaped molecules into the smectic layers creates the structural layer chirality even though the molecules are nonchiral. Phases (denoted as $B2$) with liquid-like layers and bent-shaped molecules tilted from the layer normal exhibit ferroelectric (FE) or antiferroelectric (AF) properties, similarly as the polar SmC^* phase composed of chiral rod-like molecules. As in the $B2$ phase both layer chiralities (left and right handed) are possible, either homochiral or racemic structures can be created. In racemic structures the chirality of neighboring layers regularly alternate. The bent-shaped molecules are able to form macroscopic structures with preferably AF ordering and transition between AF and FE states can be induced and switched by external electric field. The homochiral $B2$ structures are identified as anticlinic antiferroelectric (denoted as Sm$C_A P_A$) or synclinic ferroelectric (Sm$C_S P_F$) structures. The racemic structures can form synclinic antiferroelectric (Sm$C_S P_A$) and anticlinic ferroelectric (Sm$C_A P_F$) smectic structures [3].

Textures in planar samples in $B2$ phases often consist of fan-shaped and/or circular domains with complicated structure of stripes and lines of various optical contrast in polarizing microscope. Under an electric field many of stripes disappear and/or their contrast is changed [4–17]. Also reorientation of the optical axis under the electric field frequently occurs. The complicated texture and its ambiguous field behavior is a consequence of the fact that the chirality of the phase is not fixed by molecular structure and thus domains of both chiralities can coexist. Moreover, the chirality sign can be changed by the electric field (see, e.g., [2,6,8–11,14–17] and reviewed in [1,2]).

In the present contribution we will discuss our detailed observations of textures in $B2$ phases as well as particular results presented during the last decade (see e.g. [2,6,8–11,14–17]) and develop a model to explain texture behavior in external electric field. To constitute the model we will use description of walls separating domains with opposite chirality [18,19]. Detailed observations of typical textures in the $B2$ phase and their behavior in the electric field is described in Sec. II. Geometry of molecular orientation in smectic layers and relevant energies considered in our model will be outlined in Sec. III. Section IV deals with simplified model of stripe structure described in Sec. II. This model is based on a periodic system of AF domains of opposite chirality connected with π walls in which polarization rotates. The influence of an external electric field is also discussed. Finally, the interpretation of observed stripe and line textures and estimations of model parameters will be given in Sec. V. Conclusions following from the present model are given in Sec. VI.

II. OBSERVATION OF TEXTURES IN THE $B2$ PHASE

We have observed two specific types of planar textures. First type is presented by compound designed as **I** derived from naphthalene-2,7-diol-based mesogens [14] and laterally substituted by the CH_3 group. In Ref. [14] this compound was denoted as **IIj**. The other type of texture is presented by compound designed as **II**, which has the central ring connected with neighbor rings by ester linkages with methoxy substitutions on noncentral rings [13]. In Ref. [13] this compound was referred to as **4e**. Both compounds exhibit a wide temperature range AF $B2$ phase.

Generally the textures probably depend on the sample thickness, but this dependence was not specially studied. The observations were done on samples about 4 μm thick. The textures exhibit features frequently observed in the $B2$ phase formed by bent-shaped molecules [4–17]. Before an application of an external electric field both types of textures consist of high density of narrow stripes, sometimes of low contrast [Figs. 1(a) and 2(a)], which might be accompanied by sharp lines. The stripes and lines are preferentially parallel to the smectic layers. The layers are generally perpendicular to the sample surface but because of presence of focal conics

*lejcekl@fzu.cz

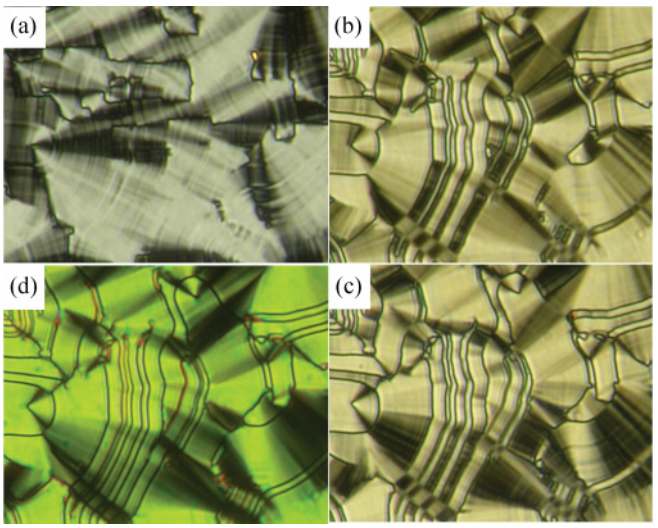

FIG. 1. (Color) Planar textures of compound **I** in the $B2$ phase observed by polarizsing microscope and changes under electric field. (a) $E = 0$, stripes of low contrast are seen. (b) $E = 15\ \mathrm{V}\,\mu\mathrm{m}^{-1}$, sharp lines are seen bordering FE domains of opposite chirality. In parts of the sample being near the extinction contrast on ferroelectric domains of opposite chirality is seen as dark and bright stripes. This contrast is interchanged for opposite field in (c) $E = -15\ \mathrm{V}\,\mu\mathrm{m}^{-1}$. (d) $E = 25\ \mathrm{V}\,\mu\mathrm{m}^{-1}$, domains of opposite chirality are not distinguishable. The contrast seen in (d) does not change for higher fields, the lines being stabilized by the field. Under the field the dark extinction brushes rotate by 45° [cf. (a) and (d)]. The width of photos corresponds to 200 μm.

they are curved. The overall texture has fan-shaped character. In crossed polarizers the parts of the samples with the stripes parallel to the direction of the light polarization are in optical extinction (dark brushes) [Figs. 1(a) and 2(a)].

Under an electric field the studied compounds exhibit different type of behavior. In compound **I** contrast of stripes is gradually fading out with the field increasing and sharp

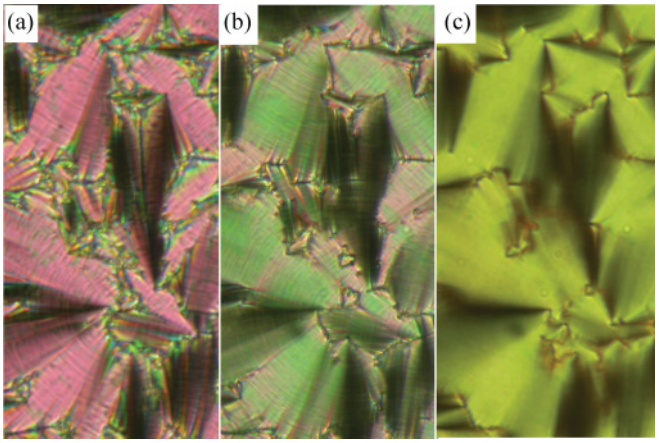

FIG. 2. (Color) Planar textures of compound **II** in the $B2$ phase observed by polarising microscope and changes under electric field. (a) $E = 0$, stripes of low contrast are seen. (b) $E = 1\ \mathrm{V}\,\mu\mathrm{m}^{-1}$ the stripes are fading out and (c) $E = 40\ \mathrm{V}\,\mu\mathrm{m}^{-1}$ no stripes lines are seen. Under the field the extinction brushes do not move. The width of photos corresponds to 150 μm.

lines appear and dominate the texture. The sharp lines do not change their positions and contrast with increasing field up to the highest applied field [see Figs. 1(b)–1(d)]. At high enough field the domains bounded by sharp lines have the same contrast at crossed polarizers [Fig. 1(d)]. Inserting λ (single wave) compensator the orientation of the optical axis could be determined, which enabled us to establish that the optical axes in the next domains are perpendicular. Under intermediate opposite fields the next stripe domains might change their contrast [cf. Figs. 1(b) and 1(c)]. This behavior will be explained below. This fact documents that the chirality of the next FE domains is opposite, similarly as it was found in Ref. [15]. Comparing Figs. 1(a) and 1(d) one can see that the extinction brushes rotate by 45° under the field showing transition from $\mathrm{Sm}C_\mathrm{A}P_\mathrm{A}$ to $\mathrm{Sm}C_\mathrm{S}P_\mathrm{F}$, both structures being homochiral and the tilt angle $\theta \approx \pi/4$. When the field decreases to zero, the stripe texture gradually reconstitutes to the same state as before the application of the electric field.

In compound **II** the stripes parallel to the smectic layers lose their contrast under the field, but sharp lines do not appear [see Figs. 2(a)–2(c)]. Besides, rotation of extinction brushes does not take place. They are still parallel to the polarization plane of polarizers. This behavior of brushes under the field cannot be directly explained by transition between the AF and FE states neither for racemic nor for homochiral state. It is necessary to consider a structure composed of domains with both chiralities [5]. A new attempt explaining this finding is given below.

Let us point out that both types of optical behavior under the field demonstrated here in details on compounds **I** and **II** have been already reported by several authors and thus can be regarded as quite typical for the $B2$ phase. The models investigated below bring a consistent explanation of behavior of defects as well as of optical properties.

III. MOLECULAR ORIENTATIONS AND ENERGY CONSIDERATIONS IN $B2$ STRUCTURES

Energy describing $B2$ structures was already discussed in detail in Refs. [18–22]. In this section, the part of the energy to be used for stripe texture model will be detailed. First, we start with general description of molecular orientation [18–20] in smectic layers of the $B2$ phase. Then the surface anchoring energy, the energy of external electric field and internal barrier energy are summarized. The internal barrier energy is the energy barrier for rotation of molecule around its long axis. Below this barrier, the bent-shaped molecules prefer to rotate on the surface of tilt cone keeping the polarization vectors within the smectic layers. Such a rotation conserves the layer chirality. Above this barrier the bent-shaped molecules can rotate also around the long molecular axis thus changing the chirality [1–5,11].

A. Molecular orientation in the smectic layers

Orientation of the bent-shaped molecule in smectic layers can be described by three Eulerian angles θ, ϕ, and ψ [23]. These angles are defined in the coordinate system with x and y axes parallel to the layers and z axis normal to the plane of layers (see Fig. 3). For simplicity, smectic layers are supposed

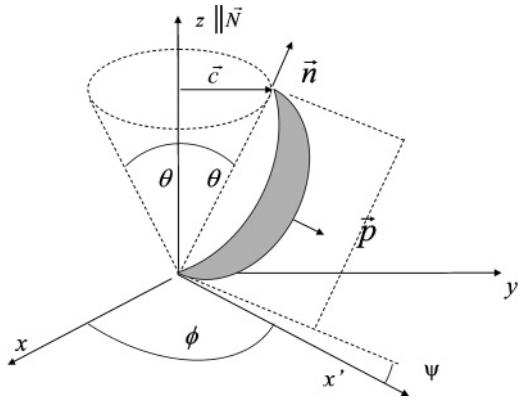

FIG. 3. The coordinate system of the bent-shaped molecule situated in the smectic layer with the normal $\vec{N}$ parallel to the z axis. The plane of the molecule (represented by a gray crescent-like object) is defined by director $\vec{n}$ and vector $\vec{p}$ parallel to molecular polarization. The $\vec{c}$ director is a projection of $\vec{n}$ onto the layer plane. Eulerian angles are defined using the coordinate system (x,y,z): θ is tilt of $\vec{n}$ from the z axis (θ is the apex angle of a cone on the surface of which the director $\vec{n}$ is located). Azimuthal angle ϕ describes rotation of $\vec{n}$ around the z axis transforming x axis to x' axis, ψ describes rotation $\vec{p}$ of around $\vec{n}$ from the x' axis. The plane of sample surface is the plane (y,z). Smectic layers are perpendicular to the sample surface and thus parallel to the plane (x,y).

to be perpendicular to the sample surfaces parallel to the (y,z) plane.

Angle θ describes the tilt of unit director $\vec{n}$ which coincides with a mean orientation of long molecular axis. The azimuthal angle ϕ characterizes the director rotation on the surface of the cone with the apex angle 2θ around the z axis. The direction of the dipole moment $\vec{p}$ of a bent-shaped molecule is perpendicular to $\vec{n}$. The angle ψ describes rotation of $\vec{p}$ around the director $\vec{n}$.

When there is no layer deformations the molecular tilt angle is constant and the molecular orientation determined by vectors $\vec{n}$ and $\vec{p}$ depends only on two variable angles ϕ and ψ [23]:

$$\begin{aligned}\vec{p} &= (\cos\theta\cos\phi\cos\psi - \sin\phi\sin\psi, \cos\theta\sin\phi\cos\psi \\ &\quad + \cos\phi\sin\psi, -\sin\theta\cos\psi), \\ \vec{n} &= (\sin\theta\cos\phi, \sin\theta\sin\phi, \cos\theta).\end{aligned} \tag{1}$$

For θ fixed, the director $\vec{c} = (\cos\phi, \sin\phi, 0)$, which is the projection of the director $\vec{n}$ onto the plane (x,y) of smectic layers, determines the molecular orientation in layers.

To describe geometrically an anticlinic AF state of the $B2$ phase we use the bilayer continuous model proposed in Refs. [22–25] for AF liquid crystals with rod-like molecules. Let us suppose that the molecular orientation is characterized by angles ϕ_1 and ψ_1 in odd-numbered layers and ϕ_2 and ψ_2 in even-numbered layers. Then we can define vectors $\vec{c}_1 = (\cos\phi_1, \sin\phi_1, 0)$, $\vec{c}_2 = (\cos\phi_2, \sin\phi_2, 0)$, and $\vec{p}_1$ and $\vec{p}_2$ using expression (1) with angles ϕ_1, ψ_1 and ϕ_2, ψ_2, respectively. Similarly as Orihara and Ishibashi [24], let us introduce vectors

$$\vec{c}_+ = \frac{\vec{c}_1 + \vec{c}_1}{2} \quad \text{and} \quad \vec{c}_- = \frac{\vec{c}_1 - \vec{c}_1}{2} \tag{2}$$

and

$$\vec{p}_+ = \frac{\vec{p}_1 + \vec{p}_1}{2} \quad \text{and} \quad \vec{c}_- = \frac{\vec{p}_1 - \vec{p}_1}{2}, \tag{3}$$

which define each of synclinic or anticlinic, FE or AF molecular structures.

B. Energies used in the model

In this subsection we will present energies used in our model describing approximately the texture behavior. The anchoring energy for both upper (+) and lower (−) sample surface can be written in the form proposed in Refs. [22,26,27]:

$$\begin{aligned}W_A = &-\gamma_1(\vec{N}_S \cdot \vec{p}_+)^2 + \gamma_2(\vec{N}_S \cdot \vec{p}_+) - \gamma_3(\vec{N}_S \cdot \vec{p}_-)^2 \\ &+ \gamma_5(\vec{N}_S \cdot \vec{c}_+)^2 + \gamma_6(\vec{N}_S \cdot \vec{c}_-)^2.\end{aligned} \tag{4}$$

Parameters γ_1 and γ_2 are anchoring constants (anchoring energies per unit surface) given by the polar molecular interaction with surfaces. Specially, the term characterized by coefficient γ_2 leads to the preferable orientation of molecular dipole toward the sample bulk center. The term characterized by coefficients γ_5 and γ_6 prefers the $\vec{c}$ director to be parallel to the sample surfaces, which corresponds either to synclinic or anticlinic molecular orientation. Vector $\vec{N}_S(\pm 1,0,0)$ is a normal to the surfaces. The upper (lower) sign corresponds to the upper (lower) surface.

For the *synclinic FE structure*, homochiral Sm$C_S P_F$, where $\phi_1 = \phi_2 = \phi$ and $\psi_1 = \psi_2 = \pi/2$ [18] the anchoring energy can be expressed as

$$W_A^{\pm} = -\gamma_1 \sin^2\phi \pm \gamma_2 \sin\phi + \gamma_5 \cos^2\phi + (\gamma_1 + \gamma_2). \tag{5}$$

The constant term $(\gamma_1 + \gamma_2)$ is added to identify local minima of Eq. (5) with the energy $W_A = 0$ for $\phi = \frac{\pi}{2}, \frac{5\pi}{2}$ (lower surface) and for $\phi = \frac{3\pi}{2}, \frac{7\pi}{2}$ (upper surface). Then the energy by which molecules are anchored to the surface is the maximum of Eq. (5).

The *anticlinic FE structure*, racemic Sm$C_A P_F$, is characterized by $\phi_1 = \pi/2, \phi_2 = 3\pi/2$ when molecules in the neighbor layers lie on the surface of the cone at opposite positions. Angles $\psi_1 = \pi/2 + \psi$ and $\psi_2 = -\pi/2 + \psi$ characterize corresponding orientations of molecular polarizations in neighbor layers. The surface energy is then

$$W_A^{\pm} = \gamma_1 \sin^2\psi + \gamma_2(1 \mp \cos\psi). \tag{6}$$

The constant term $(\gamma_1 + \gamma_2)$ was again included to assure $W_A = 0$ for $\psi = 0$ on the upper surface and for $\psi = \pi$ on the lower surface.

The energy w_E of electric field acting on the sample described by the bilayer continuous model where molecular orientation is described by angles ϕ_1, ψ_1, and ϕ_2, ψ_2, is

$$\begin{aligned}w_E = &-\tfrac{1}{2} P_S E[\cos\theta(\cos\phi_1\cos\psi_1 + \cos\phi_2\cos\psi_2) \\ &- (\sin\phi_1\sin\psi_1 + \sin\phi_2\sin\psi_2)].\end{aligned} \tag{7}$$

The parameters E and P_S in (7) are the x components of an electric field and the value of the spontaneous polarization, respectively.

For the rotation of bent-shaped molecule around director $\vec{n}$ an energetic barrier $U_b(\psi)$ proposed in Refs. [17,28] has to be overcome:

$$U_b(\psi) = U_{\max} \cos^2\theta \cos^2\psi. \tag{8}$$

Energy $U_{\max}$ ($U_{\max} > 0$) is a barrier preventing free rotation of bent-shaped molecule around the long molecular axis having the direction $\vec{n}$. Expression (8) can be identified with interaction terms $(\vec{c}_+ \cdot \vec{p}_+)^2$, $(\vec{c}_- \cdot \vec{p}_-)^2$, and $(\vec{c}_- \cdot \vec{p}_+)^2$ for synclinic FE, anticlinic AF, and anticlinic FE structures, respectively [19].

Barrier (8) can be overcome by an electric field E. When $P_S E \geqslant U_{\max}$, rotation of polarization around director $\vec{n}$ is not energetically penalized so the simultaneous rotation of molecule on the cone surface together with polarization rotation around $\vec{n}$ can occur. This effect was discussed in Refs. [1,2,4,5,12,28].

Evaluation of the energy of a wall between anticlinic AF domains of opposite chirality needs gradient elastic energy at least in some approximation. In Ref. [23] gradient orientation energy describing smectic C with orthorhombic symmetry without layer deformation is discussed. In bilayer model, when directors $\vec{c}_1$and $\vec{c}_2$ in anticlinic AF domains are fixed, that is, $\phi_1 = -\pi/2$, $\phi_2 = \pi/2$ with $\psi_1 = \psi_2 = \psi$ depending on one variable z, we obtain for one-constant approximation the gradient term of the type

$$\frac{K}{4}\left(\frac{\partial\psi}{\partial z}\right)^2.$$

We use this term as the simplest approximation of an elastic free energy density of the anticlinic AF structure in the $B2$ phase.

Chiral terms should be also considered. Principally, chiral terms

$$\frac{Kq_{cf}}{2}(\vec{c}_+ \cdot \mathrm{rot}\,\vec{c}_+), \quad \frac{Kq_{ca}}{2}(\vec{c}_- \cdot \mathrm{rot}\,\vec{c}_-),$$

and

$$\frac{Kq_{pf}}{2}(\vec{p}_+ \cdot \mathrm{rot}\,\vec{p}_+), \quad \frac{Kq_{pa}}{2}(\vec{p}_- \cdot \mathrm{rot}\,\vec{p}_-),$$

with chiral parameters q_{cf}, q_{ca}, q_{pf}, and q_{pa} lead to helical periodic structures of vectors $\vec{c}_+$, $\vec{c}_-$, $\vec{p}_+$, and $\vec{p}_-$ They can exist as they are permitted by packing of bent-shaped molecules in chiral smectic layers of the $B2$ phase.

Helical structures associated with pitches $p_{cf} = 2\pi/q_{cf}$ and $p_{ca} = 2\pi/q_{ca}$ lead principally to rotations of vectors $\vec{c}_+$ or $\vec{c}_-$, that is, to the rotations of molecular directors $\vec{n}$ on the surface of cone. The existence of such helical structures in the $B2$ phase was proved by observations of homeotropic samples with domains showing an opposite twist [29,30]. Estimations based on those observations give pitch lengths of the order of hundreds of micrometers.

The helical periodic structures of polarization vectors $\vec{p}_+$ and $\vec{p}_-$ characterized by chiral pitches p_{pf} and p_{pa} are associated with parameters $q_{pf} = 2\pi/p_{pf}$ and $q_{pa} = 2\pi/p_{pa}$, respectively. In such helical structures bent-shaped molecules rotate around their long axis parallel to the director $\vec{n}$. It means that the molecular polarization $\vec{p}$ also rotates around $\vec{n}$. Chiral parameters q_{pf} and q_{pa} are responsible for creation of a periodic system of domains of opposite chirality as proposed in [19]. As the chirality of the structure is connected with molecular configuration in smectic layers, domains differing in the sense of chirality [2,3] and thus in the sign of q_{pf} and q_{pa} can occur.

The anticlinic AF domains are described by the chiral term $\frac{Kq_{pa}}{2}(\vec{p}_- \cdot \mathrm{rot}\,\vec{p}_-)$ which can be rewritten to the form $\frac{Kq_{pa}}{2}(\frac{\partial\psi}{\partial z})$. Then the energy $\frac{K}{4}(\frac{\partial\psi}{\partial z} - q_{pa})^2$together with (8) can be used to find the solution $\psi(z)$ describing a π wall between two anticlinic AF domains of opposite chirality as it was done in Ref. [21]. This solution enables to estimate the periodicity of the system of anticlinic AF domains of opposite chiralities (see Sec. IV B).

IV. MODEL OF STRIPE TEXTURE

In this section a model of modulated structure with stripes and lines typically occurring in planar samples of the $B2$ phase [4–17] is constructed. As mentioned in Sec. II, under increasing electric field some of lines remain in the sample, while others gradually disappear. The origin of these lines as well as their behavior in the electric field has not been clarified so far. The model is based on already developed models of possible structures in the $B2$ phase [18,19,21]. As a bulk structure the chiral anticlinic AF structure $\mathrm{Sm}C_\mathrm{A}P_\mathrm{A}$ is considered. When the surface anchoring is strongly polar the AF structure near surfaces is switched to the FE one, similarly as it occurs in the AF composed of rod-like molecules [31]. Possible sample structures considered in the model are schematically shown in Fig. 4.

A. FE structures near surfaces

Let us suppose that due to the strong polar anchoring the AF structure is switched to the FE one up to distance d from surfaces. This FE structure can be either synclinic homochiral $\mathrm{Sm}C_\mathrm{S}P_\mathrm{F}$ or anticlinic racemic $\mathrm{Sm}C_\mathrm{A}P_\mathrm{F}$ (Fig. 4). These two structures will be treated separately in the following subsections.

1. Synclinic FE structure

The thickness d of the surface synclinic FE structures [Fig. 4(a)] can be estimated by comparing the maximum of anchoring energy (5),

$$W_{A\max} = \frac{[2(\gamma_1 + \gamma_5) + \gamma_2]^2}{4(\gamma_1 + \gamma_5)} \tag{9}$$

with the difference between FE and AF volume energies $-w_{C\min} = \beta_-/4$ introduced in Ref. [18]:

$$W_{A\max} = -w_{C\min} d. \tag{10}$$

The calculation gives

$$d \approx \frac{[2(\gamma_1 + \gamma_5) + \gamma_2]^2}{(\gamma_1 + \gamma_5)\beta_-}. \tag{11}$$

Parameter β_- is a coefficient of the term $(\vec{c}_- \cdot \vec{c}_-)^2/4$ in the expansion of the nongradient free energy of the $B2$ phase. In one constant approximation this term gives $-\beta_-/4$ for the anticlinic AF structure and zero for the synclinic FE structure

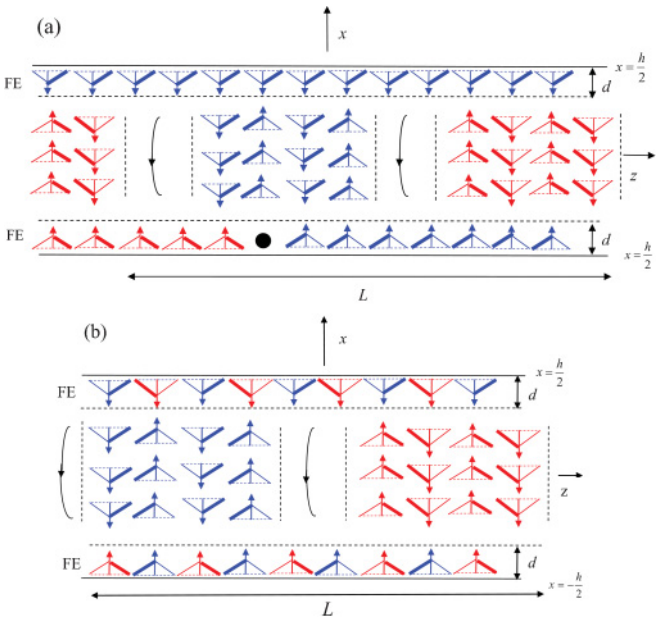

FIG. 4. (Color) Schematic representation of the sample with FE surface layers of the thickness d and AF structure in bulk. The x axis lies along smectic layers with the normal parallel to the z axis. Bent-shaped molecules are represented by triangles, dashed lines indicating projection of the director $\vec{n}$ onto the plane of the figure [(x,z) plane]. Arrows show the orientation of molecular polarization $\vec{p}$. Arms of molecules denoted by thicker lines are inclined toward the observer from the plane of figure. Thinner lines are turned behind the plane of figure. The sample thickness is h. In the sample bulk periodic system of anticlinic AF domains of opposite chirality connected by π walls along the z axis is shown. The period of the bulk system is L. Blue and red colors denote molecules of the opposite chirality. When domain and surface layer have the same chirality (same color), they can be connected by the rotation of the director $\vec{n}$ on the surface of the tilt cone. Right-handed sense of rotation of polarization vectors in π walls is selected. For the opposite chirality of the bulk domain and surface layer (different color) the rotation of both the director $\vec{n}$ on the surface of the tilt cone and the rotation of $\vec{p}$ around the director $\vec{n}$ takes place. Two configurations of surface FE layers are envisaged: (a) Synclinic FE layers at both surfaces, domains of opposite chiralities at one surface layer are separated by a surface π disclination (black dot). Walls connecting the surface FE layers and AF bulk of the same chirality are realized by rotations of $\vec{n}$. When the chirality of the surface layers differs from that of bulk AF domain the walls are realized by rotation of $\vec{p}$ around $\vec{n}$ or by the combined rotation of $\vec{n}$ and rotation of $\vec{p}$ around $\vec{n}$, in odd or even smectic layers, respectively. (b) Anticlinic FE surface layers (racemic). Both anticlinic AF bulk domains are connected with the surface layers by walls where just the rotation of $\vec{p}$ around the director $\vec{n}$ (if necessary) occurs.

[20]. Just for the comparison of energies of AF and FE states the interaction terms of vectors $\vec{c}_1$ and $\vec{c}_2$ with $\vec{p}_1$ and $\vec{p}_2$ are not important as $\psi = \pi/2$.

Surface FE structures can be of the same chirality near both surfaces or they have opposite chirality [Fig. 4(a)]. Generally, near each surface domains of opposite chirality can exist, which are separated either by a π-surface disclination, or π wall for thin or thick surface layer, respectively. Domains of opposite chirality can occur randomly in the surface FE structures. Their boundaries can be identified with the irregular surface lines observed simultaneously on both sample surfaces (see Fig. 1).

2. *Anticlinic FE structure*

The thickness d of the anticlinic FE structure near sample surfaces [Fig. 4(b)] can be estimated analogously to Eq. (11). The maximum of the anchoring energy determined from Eq. (6) is

$$W_{A\max} = \gamma_1 + \gamma_2\left(1 + \frac{\gamma_2}{4\gamma_1}\right). \tag{12}$$

Then the thickness can be estimated as

$$d \approx 4\frac{\gamma_1 + \gamma_2\left(1 + \frac{\gamma_2}{4\gamma_1}\right)}{\beta_-}. \tag{13}$$

The volume energies between FE and AF structures are the same as in previous sections. The possibility of the existence of anticlinic FE order in the sample was proved in Ref. [32] under an applied electric field. We expect the realization of the FE surface layers due to the polar anchoring. In anticlinic FE structures which are principally racemic, chiral domains cannot exist. This is the reason why no surface lines are observed in such structures.

3. *Model of stripes in bulk anticlinic AF structure*

As noted above the central part of the sample is occupied by an anticlinic AF structure. Without an electric field this central part of the sample has thickness $(h - 2d)$ where the parameter h is the sample thickness. The bulk anticlinic AF structure is supposed to have a lower energy with respect to the surface synclinic FE one stabilized by polar anchoring. Both structures can be connected by a twist wall having the thickness $\zeta_T = \sqrt{4K/\beta_-} \simeq 0.02\ \mu$m [20]. This wall is realized either by simple rotation of one of directors $\vec{c}_1$ or $\vec{c}_2$, the other being constant or rotation around the director $\vec{n}$ can be also present [see Fig. 4(a)]. The thickness d of the surface synclinic FE layer is given by Eq. (11).

Analogously, the bulk anticlinic AF structure has a lower energy with respect to the anticlinic FE structure near surfaces. The connection between these structures can be realized by the polarization rotation around the director $\vec{n}$. As for the $\vec{c}$ director, it does not change because both structures are anticlinic. The thickness of the anticlinic FE structure d is then given by Eq. (13).

The bulk structure is not influenced significantly by surface anchoring. In analogy with Ref. [21] we expect a periodic system of uniform domains of opposite chiralities in the sample bulk [Figs. 4(a) and 4(b)]. They are separated by π walls in which the molecular polarization rotates in one of two opposite senses. Therefore a complex of domains of opposite chirality separated by walls with one sense of polarization rotation forms a system having a global chirality as discussed in Ref. [21]. The driving force leading to the creation of the periodic system of domains are chiral terms characterized in the energy (3) by parameters q_{pf} and q_{pa}.

In Ref. [19] a simple case of domain π wall was discussed in anticlinic AF structures with the director $\vec{n}$ fixed at

orientations characterized by angles $\phi_1 = -\pi/2$ and $\phi_2 = \pi/2$. The angle ψ lies in the interval $(-\pi/2,\pi/2)$. The wall energy in this case [29] can be written as

$$W_S^{AF} = \frac{2K\sqrt{g_A}}{\xi},$$

where $\xi = \sqrt{K/U_{\max}}$ and the parameter g_A is situated in the interval $\cos^2\theta \leqslant g_A \leqslant 1$. The existence of walls is the consequence of the energetic barrier given by Eq. (8).

The period L of the system of anticlinic AF domains of opposite chirality was proposed in Ref. [21] where we take the value $g_A = 1$ giving us the upper value of wall energy W_S^{AF}:

$$L \approx \frac{|p_{pa}|}{1 - \frac{W_S^{AF}|p_{pa}|}{K\pi^2}} = \frac{|p_{pa}|}{1 - \frac{2|p_{pa}|}{\pi^2\xi}}. \tag{14}$$

If the periodical system of domains is observed {see Fig. 1(a) and also Refs. [1–16]}, the period L given by Eq. (14) is positive. Then the following relation should be valid:

$$|p_{pa}| < \frac{K\pi^2}{W_S^{AF}} \approx \frac{\pi^2}{2}\frac{\xi}{\sqrt{g_A}} \approx \frac{\pi^2\xi}{2}.$$

The wall energy increases the energy of the system over the period. In order to gain the energy per period the period should increase, that is, $L > |p_{pa}|$. The gain of energy is due to the chiral term. Note that for the special case when the barrier energy $U_{\max}$ is very small, that is, $U_{\max} \to 0$ then $L \to |p_{pa}|$. In this case there is not the system of domains of opposite chirality separated by walls but molecules rotate around the director continuously with the period $|p_{pa}|$ that is the chiral parameter of the liquid crystal. On the other hand, in the limit $|p_{pa}| \to \frac{K\pi^2}{W_S^{AF}}$, the period $L \to \infty$ and the system ceases to be periodic. Nevertheless, domains of opposite chirality can exist but they are distributed randomly.

The structure of π wall between two anticlinic AF structures of opposite chirality was determined in Refs. [19,21] under the simplifying assumption that the long molecular axis (along the director $\vec{n}$) is fixed and molecules in the wall just rotate around this axis. The optical contrast of such a wall is expected to be very low. On the other hand, the optical contrast of a fine line texture in Figs. 1(a) and 2(a) is dim but observable. It means that the rotation of molecules in a wall occurs not only by the rotation around $\vec{n}$ but also the $\vec{n}$ axis moves on the surface of the cone.

B. Influence of an electric field on sample structures

The field switching the bulk anticlinic AF structure is strongly influenced by the existence of FE surface layers induced by surface anchoring up to the thickness d. These layers have opposite polarization at opposite sample surfaces. The thickness of the layer having a favorable orientation of polarization with respect to the field polarity will increase thus behaving as a nucleus of FE structure for the switching of the bulk. In the following we will discuss separately the influence of an electric field on the sample having the bulk anticlinic AF structure sandwiched between either synclinic or anticlinic FE surface layers.

1. Synclinic FE surface layer in an electric field

The energy w_E of the anticlinic AF bulk structure, that is, for $\phi_1 = \phi$, $\phi_2 = \phi + \pi$, and $\psi_1 = \psi_2 = \pi/2$, is $w_E = 0$ for arbitrary ϕ. It is valid for fields lower than a critical value necessary to switch the structure to the FE one. On the other hand, the energy w_E for the synclinic FE structure, that is, for $\phi_1 = \phi_2 = \phi$, and $\psi_1 = \psi_2 = \pi/2$, is $w_E = P_S E \sin\phi$. For $P_S > 0$ and $E > 0$ the favorable synclinic FE structure is given by the molecular orientation $\phi = -\pi/2$, that is, the molecular polarization is oriented along the positive x axis.

To estimate the dependence of the surface layer thickness d on the external electric field we use relation (10) but modified by adding the energy $w_E = -P_S E$ to the energy balance, d being measured from the lower surface. This energy w_E prefers (for $E > 0$) the FE order near the lower surface where the surface polarization is oriented toward the sample center. The same energy disfavors the FE order near the upper surface where the surface polarization is oriented also toward the sample center.

The thickness of the surface layer d in low fields is calculated from the relation $W_{A\max} = -w_{C\min}d + w_E d$ as

$$d \approx \frac{\frac{[2(\gamma_1+\gamma_S)+\gamma_2]^2}{4(\gamma_1+\gamma_S)}}{\left(\frac{\beta_-}{4} - P_S E\right)}. \tag{15}$$

Equation (15) exists (i.e., d is positive) for low electric fields when $P_S E < \beta_-/4$. The field dependence of the surface layer thickness (15) [analogous to (10) without a field] was determined by comparing energy changes of FE and AF structures connected by a sharp wall of the thickness ζ_T. It demonstrates tendency of increasing the thickness of the FE structure with a favorable orientation of polarization with respect to the field polarity and its growth into the sample bulk. The preferred FE structure can propagate toward the second surface with the opposite preference of the polarization orientation. However, even on the surface with the polarization not preferred by the field the surface line persists because they are stabilized by the field [18,19]. This behavior explains why the line texture does not generally change during slow switching [cf., e.g., Figs. 1(b) and 1(c)]. On the opposite, when reversing the field polarity the thickness d decreases with the field.

2. Anticlinic FE surface layer in an electric field

When the anticlinic FE (i.e., racemic) structure exists near surfaces, expression (13) can be modified in the field similarly as Eq. (15). The energy w_E for the anticlinic FE structure, that is, for $\phi_1 = \pi/2$, $\phi_2 = 3\pi/2$, and $\psi_1 = \pi/2 + \psi$, $\psi_2 = -\pi/2 + \psi$ is $w_E = P_S E \cos\psi$. For $P_S E > 0$, the minimum energy corresponds to orientation $\psi = \pi$, that is, the molecular polarizations are oriented along the positive x- axis, which favors the FE structure near the lower sample surface. The thickness of the surface layer increases with the field and for low fields it can be approximated as

$$d \approx \frac{\gamma_1 + \gamma_2[1 + (\gamma_2/4\gamma_1)]}{\left(\frac{\beta_-}{4} - P_S E\right)}. \tag{16}$$

The increase of the thickness of the FE structure occurs at the expense of the AF structure.

V. DISCUSSION AND ESTIMATION OF MODEL PARAMETERS

Observations outlined in Sec. II, namely the observed stripe and line texture and its behavior in the electric field, can be successfully explained on the basis of the approximate model treated in Secs. IV A and IV B.

We suppose that the sample consists of three segments as schematically shown in Fig. 4: the FE structure, either synclinic [Fig. 4(a)] or anticlinic [Fig. 4(b)] near surfaces with FE order induced by polar surface interaction and the central part of the sample having the equilibrium anticlinic AF structure, not importantly influenced by polar surface interaction. The bulk and surface structures are connected by a wall [20,22].

First let us discuss the case with the *synclinic (chiral) surface layer*. It is supposed that in the FE surface layers π-surface disclinations occur [Fig. 4(a)], which may be extended to π walls for thicker surface layer, both bordering domains of opposite chirality. The director of the next domains differs by 2θ (tilt angle), which for $\theta = \pi/4$ gives no optical contrast. The disclinations should appear as contrast lines. Similarly, in the sample bulk a periodic system of π walls exists separating anticlinic AF structures of opposite chirality as schematically shown in Figs. 4(a) and 4(b). These walls are probably rather thick, so that their optical contrast is not as sharp as that of lines. The chiral bulk domains selves are not distinguished by the contrast.

The complicate irregular stripe texture as seen in Fig. 1(a) basically reflects the bulk periodic structure of chiral domains divided by walls, the width of both can be comparable. In addition, nonhomogeneous molecular structure along the sample plane normal plays a role for the optical contrast. Let us have in mind that at the upper and lower surfaces the chiral domains are overlapped and thus various combinations can be envisaged. Due to this fact the contrast of bulk stripes may be modified and additional stripes of various optical contrast may appear.

Under external electric field thickness of the preferred FE surface layer increases, while the thickness of the FE structure near the other surface with unfavorable orientation of polarization decreases. At increasing field thickness of the bulk AF structure decreases [see (15)] till the full saturated FE state. During the decrease of the bulk AF structure the optical contrast of the stripes system is fading out (cf. Fig. 1 on increasing field). Figures 1(b) and 1(c) correspond to intermediate electric fields of the opposite polarities. Switching of the field leads to switching of the optical contrast between domains of opposite chirality. The switch of the optical contrast is observed because at this field the vectors $\vec{c}_1$ and $\vec{c}_2$ are not yet parallel to the surfaces and the apparent tilt angle is then lower than $\pi/4$. It is because the wall between anticlinic AF and synclinic FE structures elastically acts again the surface polar anchoring. This can be verified by numerical model simulating approach of the apparent tilt angle to $\pi/4$ with increasing external electric field.

In the saturated FE structure the vectors $\vec{c}_1$ and $\vec{c}_2$ become parallel to the sample surfaces and the apparent tilt angle is about $\pi/4$ (for studied materials). In that case the switching of the field does not change the optical contrast of domains of opposite chirality as seen in Fig. 1(d). In Fig. 1(d) only few lines corresponding to the boundaries between domains of opposite chirality [14,17] can be seen. These lines do not change during the field switching, being stabilized on the surfaces.

For the *anticlinic (racemic) FE surface layers* the texture observed without a field exhibits a fine periodic system of stripes [see Fig. 2(a)]. Application of an electric field gradually erases this fine texture as the thickness of the surface anticlinic FE layer with preferred polarization increases and in the saturated field state this layer expands over the whole sample, which over all becomes racemic. The racemization of the sample bulk is reached by means of molecular rotation about their long axis as seen in Fig. 4(b). This rotation is possible because of relatively low energy barrier as will be discussed below. As the surface layers are racemic, no lines similar to those in Figs. 1(b)–1(d) can be formed.

The model sample structures with either synclinic or anticlinic FE surface layers enable us to explain not only both types of textures that occur in planar samples of the $B2$ phase including their behavior in the electric field, but also behavior of overall optical extinction in crossed polarizers. In the type shown in Fig. 1 the dark extinction brushes, oriented along the direction of the crossed polarizers, rotate under the electric field by the tilt angle θ to the left or right depending on the field direction. It is connected with the molecular rotation on the cone about the smectic layer normal from the field free anticlinic structure to the synclinic structure, both being chiral. In the other type as shown in Fig. 2, the extinction brushes do not rotate under the field as the field free anticlinic structure is conserved even in saturated field state.

The change of domain chirality under the field (chirality switching) has already been observed in many experiments (see, e.g., [2,6,8–11,14–17,31] and reviewed in Refs. [1,2]). In Ref. [33] it was hinted that the polarization rotation is facilitated when the layer deformation constrains the molecular rotation around the cone. Similar discussion concerning the preference of the change by the molecular rotation on the surface of the tilt cone or by chirality switching was already done in Ref. [28] showing that the mode of switching depends on the periodicity of the structure. In this study we do not discuss the influence of layer deformation on the molecular rotation and we leave it for a forthcoming study.

It should be noted that texture of the $B2$ phase in which the extinction brushes do not rotate under field was described and explained in Ref. [5] (and reviewed in Ref. [2]). The model suggested in Refs. [2,5] assumes that without a field the whole sample is in the synclinic AF (racemic) structure with domains having alternating tilt direction. Then the observed fine structure of lines could be connected with a system of anticlinic FE defects [2]. The application of an electric field transforms that structure to the anticlinic FE one, also being racemic. In the present study we expect anticlinic AF structure inside the sample which, under the field, adopts the anticlinic FE order existing at the surface due to polar anchoring. Which model realizes can depend on specific properties of liquid crystal.

The approximate model of the periodic system of anticlinic AF domains of opposite chirality presented in Sec. IV can be used for a rough estimation of various material characteristics. First, the thickness d of the surface layers can be estimated for

a field free sample. For calculation we use the elastic constant $K \approx 1.6 \times 10^{-11}$ J/m [34], the parameter $\beta_- \approx 10^5$ J/m^3 (taken from Ref. [20]) and relatively strong anchoring, characterized by parameters of anchoring energies: $\gamma_1 \approx 0.5 \times 10^{-3}$ J/m^2, $\gamma_2 \approx 10^{-3}$ J/m^2, and $\gamma_5 \approx 2 \times 10^{-3}$ J/m^2 [20]. Then the thickness of the surface synclinic FE layer can be approximately determined using expression (10) as $d \approx 0.1$ μm and for anticlinic FE layer from Eq. (13) we get $d \approx 0.07$ μm. The estimations show that even for relatively strong anchoring a predominant part of the sample remains in the AF structure, which corresponds to the equilibrium state in an infinite sample.

As already noted, in the AF bulk structure a periodic system of domains of opposite chirality occurs. From the system periodicity we can estimate a chiral parameter p_{pa}, which characterizes driving force for the structure modulation. The widths of stripes seen in Fig. 1(a) is about 1 to 2 μm. The stripes correspond to domains of opposite chirality and to walls between them having roughly the same width $\xi \approx 1 - 2$ μm as the chiral domains. The period of modulation of the AF bulk structure L, consisting of two opposite chiral domains and walls between them, can be thus estimated as $L \approx 4 - 8$ μm. Using Eq. (14) we get $p_{pa} \approx 2.2 - 4.4$ μm. For the value of energy barrier for rotation of molecules abound their axis $U_{\max} = K/\xi^2$ we get about 16 and 4 J/m^3 for $\xi \approx 1$ and 2 μm, respectively. Values $U_{\max}$ are two or four orders smaller as compared with the model values in Refs. [17,21]. The low energy barrier means that the molecular rotation around the molecular axis $\vec{n}$ is relatively easy and subsequently the thickness of the walls between chiral domains is relatively high.

As well as in the bulk, domains with opposite chirality occur also in synclinic FE surface layer. They are separated either by π disclinations or π walls, which are seen in texture as sharp lines. These lines are distant and distributed randomly confirming that chirality of this FE structure is weak.

VI. CONCLUSIONS

We have proposed possible interpretation of textures observed in the $B2$ phase formed by bent-shaped molecules and their behavior in an external electric field (Figs. 1 and 2). The textures typically exhibit lines or stripes basically parallel to the smectic layers. The reason for their orientation along the smectic layers is not discussed here because we simply suppose that it corresponds to the lowest energy. A model is proposed assuming that FE (either chiral synclinic or racemic anticlinic) structures near both sample surfaces are formed due to polar surface anchoring, the anticlinic AF structure prevailing in the sample bulk. The surface and bulk structures are mediated by walls in which the molecules rotate on the surface of the tilt cone and/or around the director $\vec{n}$ (see Fig. 4).

Domains of opposite chirality principally exist in the synclinic FE structure as well as in the anticlinic AF structure. They are separated by π-surface lines or π walls in surface FE layers and by π-domain walls in the AF bulk. The chirality of the bulk AF structure leads to creation of a periodic system of domains of opposite chirality separated by relatively thick π walls in which the polarization rotates. Basically this system represents origin of the stripe texture (Figs. 1 and 2). This system disappears simultaneously with the switching to the FE state. The irregular sharp lines correspond to walls or lines in the FE structure and thus they are stabilized under the field (Fig. 1).

The field switching to the FE phase undergoes by means of extension of the FE surface layer [either synclinic or anticlinic as seen in Figs. 4(a) or 4(b), respectively] with the dipole moment parallel to the field direction at the expense of the AF bulk structure. In the case of synclinic surface FE structure molecules rotate only on the surface of the tilt cone during switching. In the case of anticlinic surface FE structure also rotation of molecules about their long axis takes place bringing about a change of chirality. This process is enabled by rather low energetic barrier for this rotation.

Overall optical contrast at observation between crossed polarizers is given by the orientation of the optical axis of the bulk structure. The field free anticlinic AF structure exhibits extinction if polarizations of polarizers are oriented parallel and perpendicular to the smectic layer normal. This orientation rotates by the tilt angle θ when the structure is switched to the synclinic FE state under the field, rotation of extinction brushes taking place [Fig. 1 and corresponding model in Fig. 4(a)]. If the switched bulk structure becomes anticlinic FE, no rotation occurs and extinction brushes do not move [Figs. 2 and 4(b)]. The switching of the bulk structure is driven by the clinicity of the surface layer, which expands over the whole sample. In repeated experiments with various samples the type of switching manifested in optical behavior is conserved for each compound.

Generally, one can conclude that the textures of the $B2$ phase in planar samples and their changes during the electric field switching exhibit many features the details of which are characteristic for particular material. The current contribution puts forward a new sight on this issue stressing the role of polar surface anchoring. The presented model has been successful in explanation of two different behaviors of textures in the $B2$ phase of two compounds. Similar behavior has been found in many compounds so far and seems to be rather typical.

ACKNOWLEDGMENTS

This work was supported by project No. P204/11/0723 from the Grant Agency of the Czech Republic.

[1] H. Takezoe and Y. Takanishi, Jpn. J. Appl. Phys. **45**, 597 (2006).
[2] R. A. Reddy and C. Tschierske, J. Mater. Chem. **16**, 907 (2006).
[3] D. R. Link, G. Natale, R.-F. Shao, J. E. Maclennan, N. A. Clark, E. Kőrblova, and D. M. Walba, Science **278**, 1924 (1997).
[4] T. Sekine, T. Niori, J. Watanabe, T. Furukawa, S. W. Choi, and H. Takezoe, J. Mater.Chem. **7**, 1307 (1997).
[5] M. Zennyoji, Y. Takanishi, K. Ishikawa, J. Thisayukta, J. Watanabe, and H. Takezoe, J. Mater. Chem. **9**, 2775 (1999).

[6] G. Pelzl, S. Diele, S. Grande, A. Jákli, C. Lischka, H. Kresse, H. Schmalfuss, I. Wirth, and W. Weissflog, Liq. Cryst. **26**, 401 (1999).
[7] R. A. Reddy and B. K. Sadashiva, Liq. Cryst. **21**, 1613 (2000).
[8] E. Gorecka, D. Pociecha, F. Araoka, D. R. Link, M. Nakata, J. Thisayukta, Y. Takanishi, K. Ishikawa, J. Watanabe, and H. Takezoe, Phys. Rev. E **62**, R4524 (2000).
[9] S. Diez, M. R. de la Fuente, M. A. Pérez Jubindo, and B. Ros, Liq. Cryst. **301**, 1407 (2003).
[10] W. Weissflog, M. W. Schröder, S. Diele, and G. Pelzl, Adv. Mater. **15**, 630 (2003).
[11] M. W. Schröder, S. Diele, G. Pelzl, and W. Weissflog, Chem. Phys. Chem. **5**, 99 (2004).
[12] W. Weissflog, U. Dunemann, M. W. Schröder, S. Diele, G. Pelzl, H. Kresse, and S. Grande, J. Mater. Chem. **15**, 939 (2005).
[13] V. Novotná, V. Hamplova, M. Kašpar, M. Glogarová, and D. Pociecha, Liq. Cryst. **32**, 1115 (2005).
[14] V. Kozmík, A. Kovářová, M. Kuchař, J. Svoboda, V. Novotná, M. Glogarová, and J. Kroupa, Liq. Cryst. **33**, 41 (2006).
[15] C. Keith, R. A. Reddy, U. Baumeister, H. Halm, H. Lang, and C. Tschierske, J. Mater. Chem. **16**, 3444 (2006).
[16] L. E. Hough, C. Zhu, M. Nakata, N. Chattham, G. Dantlgraber, C. Tschierske, and N. A. Clark, Phys. Rev. Lett. **98**, 037802 (2007).
[17] M. Nakata, R.-F. Shao, J. E. Maclennan, W. Weissflog, and N. A. Clark, Phys Rev. Lett. **96**, 067802 (2006).
[18] L. Lejček, Liq. Cryst. **36**, 907 (2009).
[19] L. Lejček, Ferroelectrics **395**, 12 (2010).
[20] L. Lejček, V. Novotná, and M. Glogarová, Liq. Cryst. **35**, 11 (2008).
[21] L. Lejček, Phase Transitions **83**, 1001 (2010).
[22] L. Lejček, Mol. Cryst. Liq. Cryst. **494**, 21 (2008).
[23] S. Stallinga and G. Vertogen, Phys. Rev. E **49**, 1483 (1994).
[24] H. Orihara and Y. Ishibashi, Jpn. J. Appl. Phys. **29**, L115 (1990).
[25] I. Muševič, R. Blinc, and B. Žekš, *The Physics of Ferroelectric and Antiferroelectric Liquid Crystal* (World Scientific, Singapore, 2000).
[26] N. Vaupotič and M. Čopič, Phys. Rev. E **72**, 031701 (2005).
[27] H. P. Pleiner, P. E. Cladis, and H. R. Brand, Eur. Phys. J. E **20**, 257 (2006).
[28] E. Gorecka, N. Vaupotič, D. Pociecha, M. Čepič, and J. Mieczkowski, Chem. Phys. Chem. **6**, 1087 (2005).
[29] V. Kozmík, M. Kuchař, J. Svoboda, V. Novotná, M. Glogarová, U. Baumeister, S. Diele, and G. Pelzl, Liq. Cryst. **32**, 1151 (2005).
[30] M. Kohout, J. Svoboda, V. Novotná, D. Pociecha, M. Glogarová, and E. Gorecka, J. Mater. Chem. **19**, 3153 (2009).
[31] S. T. Lagerwall, *Ferroelectric and Antiferroelectric Liquid Crystal* (Wiley-VCH, Weinheim, 1999).
[32] M. Nakata, D. R. Link, F. Araoka, J. Thisayukta, Y. Takanishi, K. Ishikawa, J. Watanabe, and H. Takezoe, Liq. Cryst. **28**, 1301 (2001).
[33] M. Geese, M. Prem, and C. Tschierske, J. Mater. Chem. **206**, 9658 (2010).
[34] P. Sathyanarayana, M. Mathew, Q. Li, V. S. S. Sastry, B. Kundu, K. V. Le, H. Takezoe, and S. Dhara, Phys. Rev. E **81**, 010702 (2010).